

1 **MTS1338, a small *Mycobacterium tuberculosis* RNA, regulates** 2 **transcriptional shifts consistent with bacterial adaptation for** 3 **entering into dormancy and survival within host macrophages**

4 Elena G. Salina^{1, §}, Artem Grigorov^{2, §}, Yulia Skvortsova², Konstantin Majorov³, Oksana
5 Bychenko², Albina Ostri¹, Nadezhda Logunova³, Dmitriy Ignatov², Arseny Kaprelyants¹,
6 Alexander Apt³, Tatyana Azhikina^{2, *}

7
8 ¹ Bach Institute of Biochemistry, Research Center of Biotechnology, Moscow, Russia

9 ² Shemyakin and Ovchinnikov Institute of Bioorganic Chemistry, Moscow, Russia

10 ³ Central Institute for Tuberculosis, Moscow, Russia

11

12 * Corresponding author

13 § equally contributed to this work

14

15 **Correspondence:**

16 Tatyana L. Azhikina (tatazhik@ibch.ru)

17

18 **Keywords:** *Mycobacterium tuberculosis*; tuberculosis; small RNA; MTS1338; RNA-seq;
19 host-pathogen; infection *in vivo*; macrophages; stresses

20 **Abstract** (170 words)

21 Small non-coding RNAs play a significant role in bacterial adaptation to changing
22 environmental conditions. We investigated the dynamics of expression of MTS1338, a small
23 non-coding RNA of *Mycobacterium tuberculosis*, in the mouse model *in vivo*, regulation of
24 its expression in the *ex vivo* infected macrophages, and the consequences of its
25 overexpression in bacterial cultures. Here we demonstrate that MTS1338 significantly
26 contributes to host-pathogen interactions. Activation of the host immune system triggered
27 NO-inducible up-regulation of MTS1338 in macrophage-engulfed mycobacteria. Constitutive
28 overexpression of MTS1338 in cultured mycobacteria improved their survival *in vitro* under
29 low pH conditions. MTS1338 up-regulation launched a spectrum of shifts in the
30 transcriptome profile similar to those reported for *M. tuberculosis* adaptation to hostile intra-
31 macrophage environment. Using the RNA-seq approach, we demonstrate that gene
32 expression changes accompanying MTS1338 overexpression indicate reduction in
33 translational activity and bacterial growth, which is consistent with entering the dormant
34 state. Taken together, our results suggest a direct involvement on this sRNA in the interplay
35 between mycobacteria and the host immune system during infectious process.

36 **1. Introduction**

37 *M. tuberculosis* persistence in the infected host involves several stages and may have
38 different manifestations: initial infection followed by semi-acute or chronic diseases; latent
39 infection characterized by the presence of viable bacteria with slow-to-no level of replication
40 and the lack of clinical manifestations; and transition from the latent state to reactivation
41 processes (Russell, 2007; Stewart et al., 2003). The spectrum of the disease manifestations
42 depends upon a dynamic balance between protective host responses and defensive strategies
43 of *M. tuberculosis*. Identification of molecular mechanisms of *M. tuberculosis* adaptation to
44 the host immune defense during its persistence within macrophages is an important scientific
45 and medical problem.

46 Long co-evolution of *M. tuberculosis* and its human host allowed the pathogen to
47 develop strategies that can effectively combat host defense systems. Regulatory proteins,
48 non-coding RNAs and their targets constitute complex adaptive metabolic networks that
49 allow the pathogen to resist host response at different stages of infection. Bacterial sRNAs
50 participate in regulation of transcription and translation by affecting the level of gene
51 expression and mRNA stability. Mostly, sRNAs are expressed in response to the external
52 factors, helping bacteria to adaptively react to the changing environmental conditions and
53 regulate the key stages of pathogenesis (Dutta and Srivastava, 2018; Holmqvist and Wagner,
54 2017; Hor et al., 2018).

55 Application of the high throughput sequencing and computer algorithm approaches
56 allowed identification of dozens of sRNAs in mycobacterial species (Haning et al., 2014;
57 Schwenk and Arnvig, 2018; Taneja and Dutta, 2019). Several *in vitro* studies have elucidated
58 the functioning of sRNAs in *M. tuberculosis* (Arnvig et al., 2011; Gerrick et al., 2018;
59 Moores et al., 2017; Solans et al., 2014; Mai et al., 2019). However, dissecting the role of a
60 particular sRNA in mycobacterial physiology appeared to be difficult, especially in *in vivo*
61 settings.

62 One of such RNAs, MTS1338 (DosR-associated sRNA, ncRv11733), is highly
63 expressed during the stationary phase of growth (Arnvig and Young, 2012), and the
64 dormancy state (Ignatov et al., 2015). This sRNA is present only in genomes of highly
65 pathogenic mycobacteria and is very conservative. *In vitro* experiments demonstrated that its
66 transcription is controlled by the transcriptional regulator DosR and is activated under
67 hypoxic and NO-induced stresses (Moores et al., 2017), suggesting that MTS1338 may play a
68 role during the stable phase of infection, when host responses confront mycobacterial
69 multiplication more or less successfully. Indeed, we and others demonstrated a striking
70 increase in the MTS1338 transcription in animal models of chronic infection (Arnvig and
71 Young, 2012; Ignatov et al., 2014). Thus, it seems likely that MTS1338 triggers adaptive
72 biochemical cascades for intracellular persistence.

73 Here, we characterize the dynamic changes in the MTS1338 expression in
74 mycobacteria obtained from the lungs of genetically susceptible and resistant TB-infected
75 mice, and provide a direct evidence that the level of expression is regulated by the IFN- γ -
76 dependent NO production. Using high-throughput technologies, we describe changes in the
77 genome transcription profile that accompany an increased MTS1338 transcription.
78 Overexpression of MTS1338 leads to transcriptional shifts consistent with decreased bacterial
79 metabolism, cell division and adaptation to host immune responses experienced by
80 mycobacteria residing within host macrophages. Taken together, our results demonstrate that
81 the small non-coding MTS1338 RNA regulates molecular mechanisms providing *M.*
82 *tuberculosis* inter-macrophage survival.

83

84 **2. Materials and Methods**

85 **Bacterial strains, media and growth conditions**

86 For *in vitro* experiments, *M. tuberculosis* H37Rv, pMV (empty plasmid control) and OVER
87 (MTS1338 overexpressing) *M. tuberculosis* strains were initially grown from frozen stocks
88 for 10 days in Sauton medium. Medium content (per liter): 0.5 g KH₂PO₄, 1.4 g
89 MgSO₄×7H₂O, 4 g L-asparagine, 60 ml glycerol, 0.05 g ferric ammonium citrate, 2 g sodium
90 citrate, 0.1 ml 1% ZnSO₄, pH 7.0 (adjusted with 1M NaOH). Supplements: ADC growth
91 supplement (Connell, 1994), 0.05% Tween 80 and 50 µg/ml kanamycin (Sigma-Aldrich,
92 USA). Growth conditions: 37°C with agitation (200 rpm). The starter cultures were
93 inoculated into fresh medium (the same composition) and grown up to stationary phase for
94 RNA-seq experiments and stress survival experiments.

95 For cloning procedures, *Escherichia coli* DH5 α was grown in Luria Bertani (LB) broth and
96 LB-agar. When required, antibiotics were added at the following concentrations: kanamycin
97 (Sigma-Aldrich), 50 μ g/ml (*M. tuberculosis*); ampicillin (Invitrogen, USA), 100 μ g/ml (*E.*
98 *coli*).

99 **M. tuberculosis OVER and pMV (control) strains establishment**

100 The MTS1338 gene-containing vector was constructed on the basis of the pMV261 (Stover et
101 al., 1991) as described by (Ignatov et al., 2015). The plasmid was transferred into
102 mycobacteria by electroporation. MTS1338 overexpression was confirmed by quantitative
103 PCR. The control strain was produced using an empty pMV261 vector.

104 **Growth inhibition *in vitro* by NO, H₂O₂ and low pH**

105 Bacterial cultures were grown up to the stationary phase, washed up with PBS and diluted to
106 OD₆₀₀=0.2 (10⁷ CFU/ml) by (i) Sauton medium (pH 5.5) with ADC growth supplement and
107 0.05% Tween for low pH stress; (ii) by the culture supernatant to study inhibitory effects of
108 NO (provided by the DETA/NO donor, 0.5 mM) and H₂O₂ (10 mM). Cell viability after 24 h
109 and 48 h of stresses exposure were measured by incorporation of [³H]-uracil label. 2 μ l 5,6,-
110 [³H]-uracil (2 μ Ci) were added to 1-ml culture samples and incubated at 37°C with agitation
111 for 20 h. 200 μ l of culture were put in 3 ml 7% ice-cold CCl₃COOH, incubated at 0° C for 15
112 min and filtered through glass microfiber filters (Whatman, USA). Precipitated cells were
113 washed with 3 ml 7% CCl₃COOH and 3 ml 96% ethanol. Filters were put in 10 ml of
114 scintillation mixture; CPM were determined by LS analyser (Beckman Instruments Inc,
115 USA).

116 **RNA extraction from cultured mycobacteria**

117 Bacterial cultures were grown up to the stationary phase, rapidly cooled on ice, centrifuged,
118 and total RNA was isolated by phenol-chloroform extraction after cell disruption with Bead
119 Beater (BioSpec Products, USA) as previously described (Rustad et al., 2009). After
120 isolation, RNA was treated with Turbo DNase (Life Technologies, USA) to remove traces of
121 genomic DNA, and purified with the RNeasy mini kit (Qiagen, Netherlands). Amounts and
122 purity of RNA were determined spectrophotometrically; integrity of RNA was assessed in
123 1% agarose gel.

124 **Libraries for RNA-seq and RNA-seq data analyses**

125 RNA samples were depleted of 16S and 23S rRNA using RiboMinusTM Transcriptome
126 Isolation Kit, bacteria (Invitrogen, USA). Sequencing libraries were generated using the
127 resulting ribosomal transcript-depleted RNA and NEBNext Ultra II Directional RNA Library
128 Prep Kit (NEB, USA) according to the manufacturers' protocol. Sequencing was performed
129 using the Illumina NovaSeq as the single-ended 100 nt-long reads. Experiments were
130 performed in triplicates.

131 After quality control evaluation and trimming of bad qualitative reads the reads were mapped
132 on the reference *M. tuberculosis* genome (AL123456.3, <http://www.ncbi.nlm.nih.gov/>) by
133 Bowtie2 (Langmead and Salzberg, 2012). The alignment was performed with the "-local"
134 option, which allows leaving 5' and 3' ends uncharted. Calculation of the mapped reads for all
135 genes was performed using functions of the featureCounts package (Liao et al., 2014) built
136 into the author's script. Resulting statistics were visualized as transcription profiles using the
137 Artemis genome browser (Carver et al., 2012).

138 Differentially expressed genes were identified by the software package DESeq2 (Love et al.,
139 2014). The genes were considered to be differentially expressed, if the p-value was less than
140 0.05, the expected measure of false deviations (FDR) was not higher than 0.1, and the
141 expression change module (FC, Fold change) was not less than 3. Further distribution of
142 genes according functional categories was performed using the Mycobrowser database
143 (<https://mycobrowser.epfl.ch/>).

144 **Quantitative reverse transcription-PCR (qRT-PCR)**

145 One microgram of total RNA was used for cDNA synthesis with random hexanucleotides and
146 SuperScript III reverse transcriptase (Life Technologies, USA). Quantitative PCR was
147 performed using qPCRmix-HS SYBR (Evrogen, Russia) and the Light Cycler 480 real-time
148 PCR system (Roche, Switzerland); cycling conditions were as follows: 95°C for 20 s, 61°C
149 for 20 s, 72°C for 30 s, repeat 40 times; primers are listed in Suppl Table 1. In the end of
150 amplification, a dissociation curve was plotted to confirm specificity of the product. All real-
151 time experiments were repeated in triplicate. The results were normalized against the 16S
152 rRNA gene. Calculations were performed according to (Ganger et al., 2017) for the relative
153 expression ratio.

154 **Infections *in vivo* and *ex vivo***

155 **Mycobacteria.** For infection of mice and macrophage cultures, *M. tuberculosis* H37Rv
156 (substrain Pasteur) from the collection of CIT were used. Mycobacteria were prepared to
157 infect mice and macrophages as described previously (Lyadova et al., 2000). Briefly, to
158 obtain log-phase bacteria for challenge, 50 µl from a thawed aliquot was added to 30 ml of
159 Dubos broth (BD Bioscience, USA) supplemented with 0.5% Fatty Acid-Poor BSA
160 (Calbiochem-Behring Corp., USA) and oleic acid and incubated for 2 weeks at 37°C. The
161 resulting suspension was washed two times at 3000 g, 20 min, 4°C with Ca²⁺- and Mg²⁺-free
162 PBS containing 0,2 mM EDTA and 0,025% Tween 80. Cultures were filtered through a 45
163 µm-pore-size filter (Millipore, USA) to remove clumps. To estimate the CFU content in the
164 filtrate, 20 µl from each 5-fold serial dilution was plated onto Dubos agar (BD), and the total
165 number of micro-colonies in the spot was calculated under an inverted microscope (200^x
166 magnification) after being cultured for 3 days at 37°C. The bulk of the filtered culture was
167 stored at 4°C, and it was found that no change in the CFU content occurred during this
168 storage period.

169 **Mice.** C57BL/6Ycit (B6) and I/StSnEgYCit strain (I/St) mice were kept under conventional,
170 non-SPF conditions in the Animal Facilities of the Central Research Institute of Tuberculosis
171 (CIT, Moscow, Russia) in accordance with the guidelines from the Russian Ministry of
172 Health # 755, and under the NIH Office of Laboratory Animal Welfare (OLAW) Assurance
173 #A5502-11. Female mice aged 2.5–3.0 months were used. All experimental procedures were
174 approved by the Bioethics Committee of the Central Research Institute of Tuberculosis
175 (IACUC), protocols # 2, 3, 7, 8, 11 approved on March 6, 2016.

176 **Infection of mice.** To infect mice, mycobacteria were re-suspended in supplemented PBS.
177 Mice were infected via respiratory tract with ~100 viable CFU/mouse using an Inhalation
178 Exposure System (Glas-Col, USA), as described in (Radaeva et al., 2008; Radaeva et al.,
179 2005). The size of challenging dose was confirmed in preliminary experiments by plating
180 serial 2-fold dilutions of 2-ml homogenates of the whole lungs obtained from B6 and I/St
181 females at 2 h post-exposure onto Dubos agar and counting colonies after 3-wk incubation at
182 37°C. To assess CFU counts, lungs from individual mice were homogenized in 2.0 ml of
183 sterile saline, and 10-fold serial dilutions were plated on Dubos agar and incubated at 37°C
184 for 20-22 days.

185 **Infection of peritoneal macrophages, iNOS activation, RNA extraction.** To obtain
186 peritoneal macrophages, B6 mice were injected intra-peritoneally with 3% peptone (Sigma-
187 Aldrich) in saline. Five days later, peritoneal exudate cells (PEC) were eluted from the
188 peritoneal cavities with Ca²⁺- and Mg²⁺-free PBS supplemented with 2% FCS and 10 U/ml
189 heparin, washed twice with PBS, and resuspended in RPMI 1640 containing 5% FCS, 10 mM
190 HEPES and 2 mM L-glutamine. The content of nonspecific esterase-positive cells in PEC
191 exceeded 85 %. PEC were plated onto 90 mm Petri dishes (Costar, Corning Inc., USA) at 10
192 x 10⁶ cells/dish in 10 ml of RPMI-1640 containing 5% FCS, 10 mM HEPES and 2 mM L-
193 glutamine to obtain macrophage monolayers. The cells were allowed to adhere for 2 h at
194 37°C, 5% CO₂ before mycobacteria were added in 10 ml of supplemented RPMI-1640 at

195 MOI = 30, 20, 15 and 5 for further culturing for periods indicated in Figure 2. Macrophage-
196 free mycobacterial cultures served as controls.

197 To activate macrophages, monolayers were treated with murine rIFN- γ (100 U/ml, Sigma) for
198 14 h before adding mycobacteria. To block iNOS, 100 μ M L-NIL (Sigma) was added 1 h
199 before rIFN- γ administration.

200 To extract RNA, dishes with cell monolayers were gently shaken, culture medium was
201 completely aspirated and macrophages were lysed with 5 ml/dish of Trizol (Invitrogen) as
202 recommended by the manufacturer. Mycobacteria alone in control cultures were suspended
203 by pipetting and centrifuged at 3000 g, 20 min, 4°C. Pellets were suspended in 1 ml of Trizol.

204 **Statistics**

205 Statistical analysis was performed using ANOVA test and t-test by GraphPad Prism6.0
206 software (GraphPad Software, San Diego, CA, USA). $P < 0.05$ was considered statistically
207 significant.

208

209 **3. Results**

210 **3.1 MTS1338 expression in TB-infected mice**

211 Earlier it was demonstrated that several *M. tuberculosis* non-coding RNAs, including
212 MTS1338, are highly transcribed *in vivo* (Arnvig et al., 2011; Ignatov et al., 2014). Here, we
213 investigated the dynamical transcription profile of MTS1338 in mycobacteria extracted from
214 the mouse lungs from initial to terminal phases of infection. Aerosol infection with low doses
215 of *M. tuberculosis* leads to a chronic and temporary effectively controlled infection in
216 genetically resistant B6 mice, whilst in susceptible I/St mice fatal pulmonary pathology
217 develops relatively rapidly (Kondratieva et al., 2010). Differences in mycobacterial lung CFU
218 counts between I/St and B6 mice reached about 1.2 logs during the first 2 months post
219 challenge and remained stable until I/St mice succumbed to infection (Figure 1A). We
220 profiled the MTS1338 expression in the lung mycobacterial population by quantitative real-
221 time PCR (Figure 1B). The highest level of expression was observed at week 10 post-
222 challenge. In B6 mice, it remained high throughout the experiment, although slowly
223 decreased at the very late phase of infection. At week 10 of infection, when I/St mice start to
224 lose control of the disease progression, the level of MTS1338 expression in their lung
225 mycobacterial population was significantly higher ($P < 0.01$) than that in more resistant B6
226 mice (Figure 1B). Overall, at the stage of flourishing infection, the MTS1338 expression
227 level in the lung-residing bacteria was more than 1000-fold higher compared to its expression
228 level during stationary phase of growth *in vitro* (Ignatov et al., 2014).

229 **3.2 The expression of MTS1338 is regulated by iNOS**

230 Our *in vivo* experiments demonstrated that the level of MTS1338 expression peaks at the
231 stage of fully developed adaptive immune response against mycobacteria. At this stage, B6
232 mice display significantly higher levels of IFN- γ production compare to their I/St
233 counterparts (Logunova et al., 2015; Radaeva et al., 2005). Since IFN- γ is the key cytokine
234 activating macrophages for intracellular mycobacterial killing (Cooper, 2009), we compared
235 MTS1338 expression levels in infected peritoneal B6 macrophages, either activated by the
236 external IFN- γ , or not. The level of MTS1338 expression was assessed in dynamics at 2, 4,
237 and 24 hours of macrophage infection (Fig. 2A). In IFN- γ -activated macrophages, MTS1338
238 expression was significantly ($P < 0.001$, unpaired *t*-test) higher than in control macrophages
239 at every time point, and the difference reached more than 10-fold at 24 hours post infection.
240 Thus, pre-activation of macrophages with IFN- γ induced up-regulation of the MTS1338
241 expression in engulfed mycobacteria. Given that the efficacy of mycobacterial killing by
242 peritoneal macrophages significantly increases in the presence of IFN- γ (Majorov et al.,
243 2003), this result suggests that the level of MTS1338 expression correlates with the level of
244 pressure emanating from macrophage antibacterial systems.

245 Since the active nitrogen oxidative derivatives serve as the major trigger of MTS1338
246 transcription activation *in vitro* (Moore et al., 2017), we decided to test whether this is true
247 for the infected macrophage system. Nitrogen oxidative derivatives production in
248 macrophages depends upon inducible NO-synthase (iNOS2), thus we compared
249 mycobacteria-infected IFN- γ -activated and control macrophages cultured for 24 hours in the
250 presence or absence of L-NIL [N6-(1-iminoethyl)-L-lysine hydrochloride] – a selective
251 inhibitor of iNOS2. Inhibition of NO production in IFN- γ -activated macrophages completely
252 abrogated elevation in the MTS1338 expression. L-NIL itself did not affect MTS1338
253 expression in pure *M. tuberculosis* cultures (Figure 2B). Thus, in macrophages, nitrogen
254 oxidative derivatives are an important trigger of MTS1338 expression.

255 **3.3 Survival under *in vitro* stresses**

256 To check whether elevated transcription of MTS1338 protects *M. tuberculosis* against hostile
257 stressful environment, we compared survival of the OVER and control strains in cultures
258 subjected to different type of stresses: low pH or elevated levels of NO and H₂O₂. Inhibitory
259 effects of external NO, H₂O₂ and pH = 5.5 on mycobacteria were estimated by the level of
260 incorporation of [³H]-uracil after 24 and 48 h of stress exposure (Figure 3). In the absence of
261 stress, the OVER strain grew slightly slower than the control one ($P < 0.01$ at the 48-h time
262 point), which is consistent with earlier observations (Arnvig et al., 2011; Ignatov et al., 2015).
263 Treatment of cultures with external NO or H₂O₂ had marginal to no effect on mycobacterial
264 growth. However, overexpression of MTS1338 provided significant level of protection
265 against acidic conditions: at pH = 5.5, uracil incorporation by the OVER strain was
266 significantly higher both at 24 h ($P < 0.05$), and 48 h ($P < 0.01$) of culturing.

267 **3.4 Transcriptome changes induced by the MTS1338 overexpression are consistent with 268 mycobacterial adaptation to persistence**

269 To assess how overexpression of MTS1338 influences mycobacterial adaptation, we
270 compared transcriptomes of the OVER and control pMV strains at the phase of stationary
271 growth in liquid culture using RNA-seq approaches. The MTS1338 expression level in the
272 OVER strain in these experiments was more than 10-fold higher compared to the pMV strain
273 as confirmed by qRT-PCR (Suppl Figure 1A).

274 Mapping the processed reads against the reference *M. tuberculosis* genome
275 (AL123456.3, <http://www.ncbi.nlm.nih.gov/>), provided the following numbers of mapped
276 reads: 18940746 (96.91%), 19931958 (97.27%) and 20528207 (97.68%) for the OVER
277 strains and 18671706 (97.04%), 16003598 (96.36%) and 15540058 (96.85%) for the pMV
278 strain. The percentage of the protein-encoding part of the genome deduced from all mapped
279 reads comprised 13.97% (2609191), 20.04% (3207752) and 15.52% (2411509) for pMV, and
280 10.9% (2065273), 15.39% (3067710) and 20.11% (4127293) for OVER (12.8 x 10⁶ reads).

281 Using the software package DESeq2 (Love et al., 2014), we identified genes the
282 expression of which differed between the two strains. Unexpectedly, only 28 genes were
283 found to change their expression more than 1.5-fold under the MTS1338 overexpression
284 conditions, with 15 genes demonstrating a decreased and 13 genes an increased expression.
285 Further ascribing of genes to functional categories was performed using the Mycobrowser
286 database. The list of differentially expressed genes (DEGs) is displayed in Table 1. Complete
287 data on RNA-seq are displayed in Suppl. Table 2. Possible functional consequences of
288 particular shifts in gene expression profiles are provided in the Discussion section.
289 Differential expression of six randomly chosen genes was confirmed by the quantitative RT-
290 PCR (Suppl. Figure 1B).

291

292 **4. Discussion**

293

294 In mycobacteria, sRNAs have been discovered much later than in many other bacterial
295 species (Haning et al., 2014), and their functions mostly remain unknown. However, recent
296 high-throughput transcriptional profiling of cultured *M. tuberculosis* exposed to relevant
297 stresses identified a pool of both known and novel mycobacterial sRNAs involved in response
298 to stress conditions *in vitro* (Gerrick et al., 2018).

299 Here, we present functional characteristics of the sRNA MTS1338, one of highly
300 expressed in *M. tuberculosis* during the stationary growth phase (Arnvig et al., 2011) and at
301 dormancy (Ignatov et al., 2015), suggesting its role in the maintenance of *M. tuberculosis*
302 survival under unfavorable conditions. Since these observations suggest that high levels of
303 MTS1338 expression are required for its functional activity, we constructed the *M. tuberculosis*
304 strain overexpressing MTS1338 for identification of its *in vitro* phenotype, as well as
305 transcriptional changes triggered by this small RNA. Earlier it was demonstrated that MTS1338
306 expression is NO-inducible and is activated by transcriptional regulator DosR under hypoxic
307 cultural conditions (Moores et al., 2017), as well as under starvation, oxidative and low pH
308 stresses (Gerrick et al., 2018). Our experiments demonstrate that the strain constitutively
309 overexpressing MTS1338 is more resistant to low pH than the control strain (Figure 3).

310 Overexpression of MTS1338 dramatically changes the bacterial growth rate (Arnvig et
311 al., 2011; Ignatov et al., 2015). Our experiments with *M. tuberculosis* dormancy and
312 resuscitation *in vitro* demonstrated that MTS1338 participates in entering dormancy (Ignatov
313 et al., 2015), but is not involved in the resuscitation process (Salina et al., 2019). *In vivo*, high
314 levels of MTS1338 transcription were reported for *M. tuberculosis* residing in chronically
315 infected mouse lungs (Arnvig et al., 2011; Ignatov et al., 2014). In the present work, using a
316 mouse model of infection, we demonstrate that MTS1338 up-regulation strictly follows
317 activation of iNOS in macrophages. Importantly, at the stage of advanced infection the level of
318 expression was significantly higher in genetically TB-susceptible I/St mice compared to more
319 resistant B6 animals. This may reflect an attempt of mycobacteria residing in the I/St lungs to
320 rapidly turn down metabolism, facing severe functional failure in the surrounding tissue,
321 providing aggressive, highly hypoxic and necrotic conditions to a large proportion of
322 mycobacterial population (Kondratieva et al., 2010). We anticipated that an abundant
323 expression of MTS1338 leads to shifts of the whole genome transcriptional profile towards
324 preparation of mycobacteria to stress-induced metabolic slowdown, thereby helping survival
325 in hostile intra-macrophage surrounding

326 However, RNA-seq transcriptome evaluation demonstrated that the number of DEGs
327 in MTS1338-overexpressing and control strains is relatively small. MTS1338 overexpression
328 resulted in elevated expression of three operons – *Rv0079-Rv0081*, *Rv0082-Rv0087* and
329 *Rv1620c-Rv1622c*. *Rv0079-0081* genes belong to the DosR regulon which activates under
330 hypoxic conditions (Voskuil et al., 2003). *Rv0079* expression was shown to be regulated by
331 *Rv0081* (Chauhan et al., 2011). In *E. coli* and *M. bovis*, homologous protein significantly
332 inhibits cell growth, apparently interacting with the 30S ribosome subunit and inhibiting
333 translation – the phenotype typical for transition to dormancy (Kumar et al., 2012). *Rv0080*
334 encodes a conservative hypothetical protein with unknown functions. It contains a domain of
335 pyridoxine 5'-phosphate (PNP) oxidase-like (PNPOx-like) superfamily, which catalyze flavin
336 mononucleotide-mediated redox reactions. *Rv0081* is one of two key transcriptional factors
337 mediating early response to hypoxia (Galagan et al., 2013). As an important “metabolic hub”
338 working in concert with other transcription regulators, *Rv0081* is associated with the processes
339 of lipid metabolism, protein degradation and cholesterol biosynthesis.

340 The genes of other two operons encode proteins of the functional category
341 “Intermediary metabolism and respiration”. *Rv0082-Rv0087* genes are also regulated by
342 *Rv0081* (He et al., 2011), but not included in the DosR regulon. The *Rv0082–Rv0087* locus in
343 *M. tuberculosis* encodes a putative [NiFe]-hydrogenase complex (Berney et al., 2014). In *E.*
344 *coli*, homologous proteins are involved in the conversion of formate to CO₂ and H₂ under
345 conditions of anaerobic respiration in the absence of an external terminal electron acceptor
346 (Leonhartsberger et al., 2002). Facultative H₂ metabolism is central for mycobacterial
347 persistence. Mycobacteria enhance long-term survival by up-regulating hydrogenases during
348 energy and oxygen limitations (Greening and Cook, 2014).

349 *Rv1620c-Rv1622c* (*cydC*, *D*, *B* respectively) encode proteins, which are involved in the
350 cytochrome biogenesis and active transport across the membrane of components involved in
351 the assembly of cytochrome. The expression of *CydDC* is linked to the incorporation of heme
352 cofactors into a variety of periplasmic cytochromes, as well as the bd-type respiratory oxidases.
353 *CydB* is the component of the aerobic respiratory chain that is supposedly predominant when
354 cells are grown at low aeration, and is up-regulated under low pH (Baker et al., 2014). It has
355 been reported that the presence of bd-type oxidases is correlated with bacterial virulence. For
356 example, growth of mycobacteria at low oxygen tensions enhances both the expression of a
357 bd-type oxidase and cell invasion (Bermudez et al., 1997).

358 Down-regulated genes belong to different functional categories. Among them, three
359 genes with chaperone functions attract special attention. All these genes are essential for *M.*
360 *tuberculosis* growth *in vitro* (Griffin et al., 2011; Sassetti et al., 2003). *Rv0440* encodes
361 GroEL2, the chaperone belonging to the HSP60 family. Its chaperone-like functions provide
362 resistance to stress (Qamra et al., 2004) and modulate host immune responses (Lewthwaite et
363 al., 2007; Naffin-Olivos et al., 2014). GroEL2 is highly induced in response to environmental
364 cues during infection like heat shock, oxidative stress, growth in macrophages and hypoxia
365 (Qamra et al., 2005). The HupB protein encoded by *Rv2986c* belongs to the histone-like family
366 of prokaryotic DNA-binding proteins capable of wrapping DNA to stabilize it, and prevent
367 DNA denaturation under extreme environmental conditions (Kumar et al., 2010). It is involved
368 in controlling the transfer of mycolic acids to sugars by the Ag85 complex (Katsube et al.,
369 2007), as well as siderophore biosynthesis, and is essential for mycobacteria growth in
370 macrophages (Pandey et al., 2014).

371 *WhiB2* encoded by *Rv3260c* belongs to the *WhiB* family of transcriptional regulators.
372 Its apo-form displays a chaperone activity, preventing aggregation and providing correct
373 refolding of proteins; this activity does not require ATP and is independent of its own oxidized
374 or reduced status and co-chaperones (Konar et al., 2012). The homologue of *whiB2* in *M.*
375 *smegmatis*, *WhmD*, participates in septa formation during cell division. *WhmD*
376 overexpression decreases the linear size of *M. smegmatis* cells (Raghunand and Bishai, 2006).
377 In addition, the newly formed cell walls are more susceptible to lysis (Gomez and Bishai,
378 2000). It was suggested that *WhiB2* is involved in the assembly and stabilization of the FtsZ
379 ring around the cell septum during division (Huang et al., 2013).

380 Two other down-regulated genes, *Rv2987c* and *Rv2988c*, encode subunits of putative
381 3-isopropylmalate dehydratase and are involved in leucine biosynthesis. *In vivo* and *in vitro*
382 studies demonstrate that leucine-auxotrophic *M. tuberculosis* strains do not replicate inside host
383 cells (Hondalus et al., 2000).

384 Overall, up-regulated genes fall into “intermediate metabolism and respiration”
385 functional category, and either belong to the DosR regulon directly (*Rv0079-Rv0081*), or are

386 connected through DosR-regulated transcriptional factor *Rv0081* (*Rv0082-Rv0087*). All up-
387 regulated genes are thought to be involved into mycobacterial survival inside macrophages.

388 The list of down-regulated genes is functionally more diverse. Of interest is a decreased
389 of genes encoding chaperone proteins, such as GroEL2, HupB, WhiB2. Theoretically, their
390 expression should be rather increased under unfavorable conditions. To find an explanation of
391 this paradox, we studied TB databases (<http://genome.tdb.org>), concentrating on groups of
392 genes co-expressed with these chaperones genes. It appeared that the majority of DEGs,
393 including *groEL2*, *hupB* and *whiB2*, are co-expressed with genes of the functional category J:
394 Translation, ribosomal structure and biogenesis (Clusters of Orthologous Groups, COG,
395 (Tatusov et al., 2000)). In all cases, irrespective to up- or down-regulation of DEGs, there was
396 reversed correlation with genes of the J category (Table 2). These data suggest that the
397 MTS1338 overexpression leads to transcriptional changes that correlate with a translation
398 slowdown.

399 Summarizing, our results suggest an important potential role of MTS1338 in
400 pathogenesis of mycobacteria-triggered diseases. An increase in MTS1338 production during
401 infection *in vivo* and in activated macrophages, changes in the expression of genes important
402 for mycobacterial metabolism and a better survival under low pH accompanying MTS1338
403 overexpression – all suggest that this sRNA may well contribute to successful persistence of
404 *M. tuberculosis* within host cells.

405 406 **Acknowledgements**

407 This work was supported by the Russian Science Foundation grant №18-15-00332 to TA
408 (new MTb strains, RNA-seq experiments and analyses, stresses *in vitro*); grant №18-45-
409 04015 to AA (in vivo and ex vivo infection experiments)

410 411 **Authors contribution**

412 Conceived the idea and designed the experiments: EGS, DI, AK, AA, TA. Performed the
413 experiments: EGS, AG, YS, KM, OB, AO, NL. Analyzed the data: EGS, AK, AA, TA. Wrote
414 the paper: EGS, AK, AA, TA.

415 416 **Conflict of Interest**

417 Authors declare no conflict of interests.

418 419 **Data availability statement**

420 The data sets supporting the results of this article are available in the GEO data repository
421 under the accession number GSE137857.

422 423 424 **References**

- 425
426 Arnvig, K., and Young, D. (2012). Non-coding RNA and its potential role in Mycobacterium
427 tuberculosis pathogenesis. *RNA Biol.* 9, 427-36. doi: 10.4161/rna.20105
428 Arnvig, K.B., Comas, I., Thomson, N.R., Houghton, J., Boshoff, H.I., Croucher, N.J., et al.
429 (2011). Sequence-based analysis uncovers an abundance of non-coding RNA in the
430 total transcriptome of Mycobacterium tuberculosis. *PLoS Pathog.* 7, e1002342. doi:
431 10.1371/journal.ppat.1002342
432 Baker, J.J., Johnson, B.K., and Abramovitch, R.B. (2014). Slow growth of Mycobacterium
433 tuberculosis at acidic pH is regulated by phoPR and host-associated carbon sources.
434 *Mol Microbiol.* 94, 56-69. doi: 10.1111/mmi.12688

- 435 Bermudez, L.E., Petrofsky, M., and Goodman, J. (1997). Exposure to low oxygen tension and
436 increased osmolarity enhance the ability of *Mycobacterium avium* to enter intestinal
437 epithelial (HT-29) cells. *Infect Immun.* 65, 3768-73
- 438 Berney, M., Greening, C., Hards, K., Collins, D., and Cook, G.M. (2014). Three different
439 [NiFe] hydrogenases confer metabolic flexibility in the obligate aerobe
440 *Mycobacterium smegmatis*. *Environ Microbiol.* 16, 318-30
- 441 Carver, T., Harris, S.R., Berriman, M., Parkhill, J., and McQuillan, J.A. (2012). Artemis: an
442 integrated platform for visualization and analysis of high-throughput sequence-based
443 experimental data. *Bioinformatics.* 28, 464-9. doi: 10.1093/bioinformatics/btr703
- 444 Chauhan, S., Sharma, D., Singh, A., Surolia, A., and Tyagi, J.S. (2011). Comprehensive
445 insights into *Mycobacterium tuberculosis* DevR (DosR) regulon activation switch.
446 *Nucleic Acids Res.* 39, 7400-14. doi: 10.1093/nar/gkr375
- 447 Connell, N.D. (1994). *Mycobacterium*: isolation, maintenance, transformation, and mutant
448 selection. *Methods Cell Biol.* 45, 107-25
- 449 Cooper, A.M. (2009). Cell-mediated immune responses in tuberculosis. *Annu Rev Immunol.*
450 27, 393-422. doi: 10.1146/annurev.immunol.021908.132703
- 451 Dutta, T., and Srivastava, S. (2018). Small RNA-mediated regulation in bacteria: A growing
452 palette of diverse mechanisms. *Gene.* 656, 60-72. doi: 10.1016/j.gene.2018.02.068
- 453 Galagan, J.E., Minch, K., Peterson, M., Lyubetskaya, A., Azizi, E., Sweet, L., et al. (2013).
454 The *Mycobacterium tuberculosis* regulatory network and hypoxia. *Nature.* 499, 178-
455 83. doi: 10.1038/nature12337
- 456 Ganger, M.T., Dietz, G.D., and Ewing, S.J. (2017). A common base method for analysis of
457 qPCR data and the application of simple blocking in qPCR experiments. *BMC*
458 *Bioinformatics.* 18, 534. doi: 10.1186/s12859-017-1949-5
- 459 Gerrick, E.R., Barbier, T., Chase, M.R., Xu, R., Francois, J., Lin, V.H., et al. (2018). Small
460 RNA profiling in *Mycobacterium tuberculosis* identifies MrsI as necessary for an
461 anticipatory iron sparing response. *Proc Natl Acad Sci U S A.* 115, 6464-6469. doi:
462 10.1073/pnas.1718003115
- 463 Greening, C., and Cook, G.M. (2014). Integration of hydrogenase expression and hydrogen
464 sensing in bacterial cell physiology. *Curr Opin Microbiol.* 18, 30-8. doi:
465 10.1016/j.mib.2014.02.001
- 466 Haning, K., Cho, S.H., and Contreras, L.M. (2014). Small RNAs in mycobacteria: an
467 unfolding story. *Front Cell Infect Microbiol.* 4, 96. doi: 10.3389/fcimb.2014.00096
- 468 He, H., Bretl, D.J., Penoske, R.M., Anderson, D.M., and Zahrt, T.C. (2011). Components of
469 the Rv0081-Rv0088 locus, which encodes a predicted formate hydrogenlyase
470 complex, are coregulated by Rv0081, MprA, and DosR in *Mycobacterium*
471 *tuberculosis*. *J Bacteriol.* 193, 5105-18. doi: 10.1128/JB.05562-11
- 472 Holmqvist, E., and Wagner, E.G.H. (2017). Impact of bacterial sRNAs in stress responses.
473 *Biochem Soc Trans.* 45, 1203-1212. doi: 10.1042/BST20160363
- 474 Hor, J., Gorski, S.A., and Vogel, J. (2018). Bacterial RNA Biology on a Genome Scale. *Mol*
475 *Cell.* 70, 785-799. doi: 10.1016/j.molcel.2017.12.023
- 476 Ignatov, D.V., Salina, E.G., Fursov, M.V., Skvortsov, T.A., Azhikina, T.L., and Kaprelyants,
477 A.S. (2015). Dormant non-culturable *Mycobacterium tuberculosis* retains stable low-
478 abundant mRNA. *BMC Genomics.* 16, 954. doi: 10.1186/s12864-015-2197-6
- 479 Ignatov, D.V., Timoshina, O.Y., Logunova, N.N., Skvortsov, T.A., and Azhikina, T.L.
480 (2014). Expression of Small RNAs of *Mycobacterium tuberculosis* in Murine Models
481 of Tuberculosis Infection. *Russian Journal of Bioorganic Chemistry.* 40, 233-235. doi:
482 10.1134/S1068162014020058

- 483 Katsube, T., Matsumoto, S., Takatsuka, M., Okuyama, M., Ozeki, Y., Naito, M., et al. (2007).
484 Control of cell wall assembly by a histone-like protein in Mycobacteria. *J Bacteriol.*
485 189, 8241-9. doi: 10.1128/JB.00550-07
- 486 Kondratieva, E., Logunova, N., Majorov, K., Averbakh, M., and Apt, A. (2010). Host
487 genetics in granuloma formation: human-like lung pathology in mice with reciprocal
488 genetic susceptibility to *M. tuberculosis* and *M. avium*. *PLoS One.* 5, e10515. doi:
489 10.1371/journal.pone.0010515
- 490 Kumar, A., Majid, M., Kunisch, R., Rani, P.S., Qureshi, I.A., Lewin, A., et al. (2012).
491 *Mycobacterium tuberculosis* DosR regulon gene Rv0079 encodes a putative,
492 'dormancy associated translation inhibitor (DATIN)'. *PLoS One.* 7, e38709. doi:
493 10.1371/journal.pone.0038709
- 494 Langmead, B., and Salzberg, S.L. (2012). Fast gapped-read alignment with Bowtie 2. *Nat*
495 *Methods.* 9, 357-9. doi: 10.1038/nmeth.1923
- 496 Leonhartsberger, S., Korsá, I., and Bock, A. (2002). The molecular biology of formate
497 metabolism in enterobacteria. *J Mol Microbiol Biotechnol.* 4, 269-76
- 498 Liao, Y., Smyth, G.K., and Shi, W. (2014). featureCounts: an efficient general purpose
499 program for assigning sequence reads to genomic features. *Bioinformatics.* 30, 923-
500 30. doi: 10.1093/bioinformatics/btt656
- 501 Logunova, N., Korotetskaya, M., Polshakov, V., and Apt, A. (2015). The QTL within the H2
502 Complex Involved in the Control of Tuberculosis Infection in Mice Is the Classical
503 Class II H2-Ab1 Gene. *PLoS Genet.* 11, e1005672. doi:
504 10.1371/journal.pgen.1005672
- 505 Love, M.I., Huber, W., and Anders, S. (2014). Moderated estimation of fold change and
506 dispersion for RNA-seq data with DESeq2. *Genome Biol.* 15, 550. doi:
507 10.1186/s13059-014-0550-8
- 508 Lyadova, I.V., Eruslanov, E.B., Khaidukov, S.V., Yermeev, V.V., Majorov, K.B., Pichugin,
509 A.V., et al. (2000). Comparative analysis of T lymphocytes recovered from the lungs
510 of mice genetically susceptible, resistant, and hyperresistant to *Mycobacterium*
511 *tuberculosis*-triggered disease. *J Immunol.* 165, 5921-31
- 512 Mai, J., Rao, C., Watt, J., Sun, X., Lin, C., Zhang, L., et al. (2019). *Mycobacterium*
513 *tuberculosis* 6C sRNA binds multiple mRNA targets via C-rich loops independent of
514 RNA chaperones. *Nucleic Acids Res.* 47, 4292-4307. doi: 10.1093/nar/gkz149
- 515 Majorov, K.B., Lyadova, I.V., Kondratieva, T.K., Eruslanov, E.B., Rubakova, E.I., Orlova,
516 M.O., et al. (2003). Different innate ability of I/St and A/Sn mice to combat virulent
517 *Mycobacterium tuberculosis*: phenotypes expressed in lung and extrapulmonary
518 macrophages. *Infect Immun.* 71, 697-707. doi:
519 10.1128/IAI.71.3.697-707.2003
- 520 Moores, A., Riesco, A.B., Schwenk, S., and Arnvig, K.B. (2017). Expression, maturation and
521 turnover of DrrS, an unusually stable, DosR regulated small RNA in *Mycobacterium*
522 *tuberculosis*. *PLoS One.* 12, e0174079. doi: 10.1371/journal.pone.0174079
- 523 Radaeva, T.V., Kondratieva, E.V., Sosunov, V.V., Majorov, K.B., and Apt, A. (2008). A
524 human-like TB in genetically susceptible mice followed by the true dormancy in a
525 Cornell-like model. *Tuberculosis (Edinb).* 88, 576-85. doi:
526 10.1016/j.tube.2008.05.003
- 527 Radaeva, T.V., Nikonenko, B.V., Mischenko, V.V., Averbakh, M.M., Jr., and Apt, A.S.
528 (2005). Direct comparison of low-dose and Cornell-like models of chronic and
529 reactivation tuberculosis in genetically susceptible I/St and resistant B6 mice.
530 *Tuberculosis (Edinb).* 85, 65-72. doi: 10.1016/j.tube.2004.09.014
- 531 Russell, D.G. (2007). Who puts the tubercle in tuberculosis? *Nat Rev Microbiol.* 5, 39-47.
doi: 10.1038/nrmicro1538

- 532 Rustad, T.R., Roberts, D.M., Liao, R.P., and Sherman, D.R. (2009). Isolation of
533 mycobacterial RNA. *Methods Mol Biol.* 465, 13-21. doi: 10.1007/978-1-59745-207-
534 6_2
- 535 Schwenk, S., and Arnvig, K.B. (2018). Regulatory RNA in *Mycobacterium tuberculosis*,
536 back to basics. *Pathog Dis.* 76, doi: 10.1093/femspd/fty035
- 537 Solans, L., Gonzalo-Asensio, J., Sala, C., Benjak, A., Uplekar, S., Rougemont, J., et al.
538 (2014). The PhoP-dependent ncRNA Mcr7 modulates the TAT secretion system in
539 *Mycobacterium tuberculosis*. *PLoS Pathog.* 10, e1004183. doi:
540 10.1371/journal.ppat.1004183
- 541 Stewart, G.R., Robertson, B.D., and Young, D.B. (2003). Tuberculosis: a problem with
542 persistence. *Nat Rev Microbiol.* 1, 97-105. doi: 10.1038/nrmicro749
- 543 Stover, C.K., de la Cruz, V.F., Fuerst, T.R., Burlein, J.E., Benson, L.A., Bennett, L.T., et al.
544 (1991). New use of BCG for recombinant vaccines. *Nature.* 351, 456-60. doi:
545 10.1038/351456a0
- 546 Taneja, S., and Dutta, T. (2019). On a stake-out: Mycobacterial small RNA identification and
547 regulation. *Non-coding RNA Research.* doi: 10.1016/j.ncrna.2019.05.001
- 548 Tatusov, R.L., Galperin, M.Y., Natale, D.A., and Koonin, E.V. (2000). The COG database: a
549 tool for genome-scale analysis of protein functions and evolution. *Nucleic Acids Res.*
550 28, 33-6. doi: 10.1093/nar/28.1.33
- 551 Voskuil, M.I., Schnappinger, D., Visconti, K.C., Harrell, M.I., Dolganov, G.M., Sherman,
552 D.R., et al. (2003). Inhibition of respiration by nitric oxide induces a *Mycobacterium*
553 *tuberculosis* dormancy program. *J Exp Med.* 198, 705-13. doi: 10.1084/jem.20030205
- 554
555
556

557 **Legends to figures**

558 **Figure 1. *M. tuberculosis* infection in resistant B6 and susceptible I/St mice**

559 (A). Lung CFU counts along the disease progression (** $P < 0.01$ at 5- and 10-weeks post
560 challenge, ANOVA). (B). MTS1338 expression levels of at different time points. (** $P < 0.01$
561 and *** $P < 0.001$, unpaired t -test). At indicated time points, samples of total RNA were
562 analyzed by quantitative real-time PCR, and the MTS1338 expression levels in the lung
563 tissue were normalized to those of 16S rRNA. The data are presented as the mean \pm SD of
564 three independent experiments.

565

566 **Figure 2. MTS1338 transcription is NO-dependent and correlates with activation of
567 infected macrophages.**

568 (A). The MTS1338 transcription dynamics in infected peritoneal macrophages of B6 mice.
569 (B). The level of MTS1338 transcription at 24 h post infection: control (m ϕ +MTb), IFN- γ -
570 activated (m ϕ +MTb + INF- γ), IFN- γ -activated and L-NIL treated (m ϕ +MTb + INF- γ +
571 NIL). The levels of MTS1338 transcription in pure *M. tuberculosis* cultures (MTb) and L-
572 NIL-treated cultures (MTb + NIL) serve as controls for the assessment of possible L-NIL
573 influence onto cultured mycobacteria. The data are presented as the mean \pm SD of three
574 independent experiments; ** $P < 0.01$, *** $P < 0.005$, ns – not significant, unpaired t -test).

575

576 **Figure 3. Viability of the OVER and control *M. tuberculosis* strains under stressful
577 conditions in vitro.**

578 Stationary phase mycobacteria were subjected to pH = 5.5 or elevated levels of NO and H₂O₂
579 in 24-h and 48-h cultures. The effect of stresses was measured by [³H]-uracil incorporation in
580 three independent experiments and expresses as mean CPM \pm SD. * $P < 0.05$, ** $P < 0.01$,
581 unpaired t -test).

582 The data are presented as the mean \pm SD of three independent experiments.

583

584 **Supplementary material**

585 **Supp Table 1. Oligonucleotides used in the study**

586 **Suppl Table 2. RNA-seq data**

587

588

589

590 Table 1. List of genes, differentially expressed in OVER strain vs pMV strain

| <i>Gene</i> | | Function (according to Mycobrowser) | Functional category | Essentiality in vitro (Griffin et al., 2011; Sasseti et al., 2003) | Fold Change |
|----------------|---------------|---|---|--|-------------|
| <i>Rv0079</i> | | | Conserved hypotheticals | | 8,2 |
| <i>Rv0080</i> | | | Conserved hypotheticals | | 10,0 |
| <i>Rv0081</i> | | | Regulatory proteins | | 4,9 |
| <i>Rv0082</i> | | Probable oxidoreductase | Intermediary metabolism and respiration | | 6,1 |
| <i>Rv0083</i> | | Probable oxidoreductase | Intermediary metabolism and respiration | | 5,7 |
| <i>Rv0084</i> | <i>hycD</i> | Possible formate hydrogenlyase HycD | Intermediary metabolism and respiration | | 4,0 |
| <i>Rv0085</i> | <i>hycP</i> | Possible hydrogenase HycP | Intermediary metabolism and respiration | ES | 6,2 |
| <i>Rv0086</i> | <i>hycQ</i> | Possible hydrogenase HycQ | Intermediary metabolism and respiration | ES | 5,2 |
| <i>Rv0087</i> | <i>hycE</i> | Possible formate hydrogenase HycE | Intermediary metabolism and respiration | | 4,2 |
| <i>Rv0440</i> | <i>groEL2</i> | 60 kDa chaperonin 2 GroEL2 (protein CPN60-2) (GroEL protein 2) (65 kDa antigen) (heat shock protein 65) (cell wall protein A) (antigen A) | Virulence, detoxification, adaptation | ES | 0,2 |
| <i>Rv0516c</i> | | Possible anti-anti-sigma factor | Information pathways | | 2,9 |
| <i>Rv1158c</i> | | Conserved hypothetical ala-, pro-rich protein | Conserved hypotheticals | | 0,05 |
| <i>Rv1469</i> | <i>ctpD</i> | Probable cation transporter P-type ATPase D CtpD | Cell wall and cell processes | | 0,4 |
| <i>Rv1620c</i> | <i>cydC</i> | Probable 'component linked with the assembly of cytochrome' transport transmembrane ATP-binding protein ABC transporter CydC | Intermediary metabolism and respiration | ES | 7,4 |
| <i>Rv1621c</i> | <i>cydD</i> | Probable 'component linked with the assembly of cytochrome' transport transmembrane ATP-binding protein ABC transporter CydD | Intermediary metabolism and respiration | | 5,7 |
| <i>Rv1622c</i> | <i>cydB</i> | Probable integral membrane cytochrome D ubiquinol oxidase (subunit II) CydB (cytochrome BD-I oxidase subunit II) | Intermediary metabolism and respiration | ES | 5,7 |
| <i>Rv1690</i> | <i>lprJ</i> | Probable lipoprotein LprJ | Cell wall and cell processes | | 0,3 |

| | | | | | |
|----------------|--------------|--|---|----|-----|
| <i>Rv1772</i> | | | Conserved hypotheticals | | 0,3 |
| <i>Rv2033c</i> | | | Conserved hypotheticals | | 0,2 |
| <i>Rv2812</i> | | Probable transposase | Insertion seqs and phages | | 0,1 |
| <i>Rv2947c</i> | <i>pks15</i> | Probable polyketide synthase Pks15 | Lipid metabolism | | 0,2 |
| <i>Rv2986c</i> | <i>hupB</i> | DNA-binding protein HU homolog HupB (histone-like protein) (HLP) (21-kDa laminin-2-binding protein) | Information pathways | ES | 0,2 |
| <i>Rv2987c</i> | <i>leuD</i> | Probable 3-isopropylmalate dehydratase (small subunit) LeuD (isopropylmalate isomerase) (alpha-IPM isomerase) (IPMI) | Intermediary metabolism and respiration | ES | 0,2 |
| <i>Rv2988c</i> | <i>leuC</i> | Probable 3-isopropylmalate dehydratase (large subunit) LeuC (isopropylmalate isomerase) (alpha-IPM isomerase) (IPMI) | Intermediary metabolism and respiration | | 0,3 |
| <i>Rv3019c</i> | <i>esxR</i> | Secreted ESAT-6 like protein EsxR (TB10.3) (ESAT-6 like protein 9) | Cell wall and cell processes | | 0,3 |
| <i>Rv3136</i> | <i>PPE51</i> | PPE family protein PPE51 | Pe/ppe | | 0,1 |
| <i>Rv3260c</i> | <i>whiB2</i> | Probable transcriptional regulatory protein WhiB-like WhiB2 | Regulatory proteins | ES | 0,2 |
| <i>Rv3767c</i> | | Possible S-adenosylmethionine-dependent methyltransferase | Lipid metabolism | | 0,3 |

591

592

593

594

595

596

597

598

599

600 Table 2. DEGs, and their correlation with expression of different functional categories
 601 (according to COG)
 602 abbreviations: C – energy production and conversion; J - Translation, ribosomal structure and
 603 biogenesis; K – transcription; M - cell envelope biogenesis, outer membrane; O -
 604 posttranslational modifications, protein turnover, chaperones; T - signal transduction
 605 mechanisms. Orange boxes stand for up-regulated DEGs, green – down-regulated DEGs.
 606

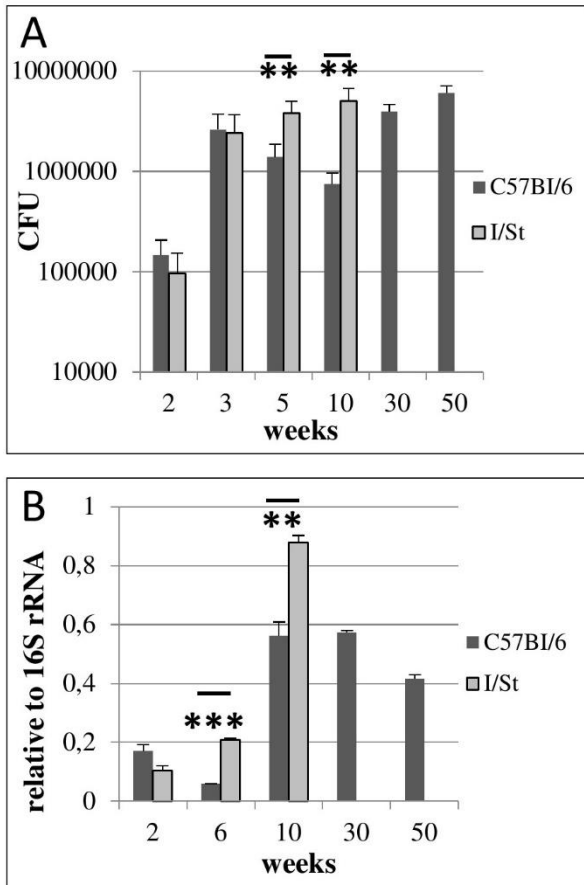
| gene | | product | Genes with correlated expression, categories enriched | |
|----------------|----------------|--|---|----------------------|
| | | | Positive correlation | Negative correlation |
| <i>Rv0079</i> | <i>Rv0079</i> | | T | |
| <i>Rv0080</i> | <i>Rv0080</i> | | T | C, J |
| <i>Rv0087</i> | <i>hycE</i> | Possible formate hydrogenase HycE | | J |
| <i>Rv0440</i> | <i>groEL2</i> | 60 kDa chaperonin 2 GroEL2 | J | |
| <i>Rv1158c</i> | <i>Rv1158c</i> | Conserved hypothetical ala-, pro-rich protein | C, M | |
| <i>Rv1620c</i> | <i>cydC</i> | Probable 'component linked with the assembly of cytochrome' transport transmembrane ATP-binding protein ABC transporter CydC | | J |
| <i>Rv1621c</i> | <i>cydD</i> | Probable 'component linked with the assembly of cytochrome' transport transmembrane ATP-binding protein ABC transporter CydD | | J |
| <i>Rv1622c</i> | <i>cydB</i> | Probable integral membrane cytochrome D ubiquinol oxidase (subunit II) CydB (cytochrome BD-I oxidase subunit II) | | J |
| <i>Rv2947c</i> | <i>pks15</i> | Probable polyketide synthase Pks15 | J | K |
| <i>Rv2986c</i> | <i>hupB</i> | DNA-binding protein HU homolog HupB (histone-like protein) | J | |
| <i>Rv2988c</i> | <i>leuC</i> | Probable 3-isopropylmalate dehydratase (large subunit) LeuC (isopropylmalate isomerase) (alpha-IPM isomerase) (IPMI) | K | |
| <i>Rv3019c</i> | <i>esxR</i> | Secreted ESAT-6 like protein EsxR (TB10.3) (ESAT-6 like protein 9) | C, O | |
| <i>Rv3136</i> | <i>PPE51</i> | PPE family protein PPE51 | J | |

607

608

609

610



611

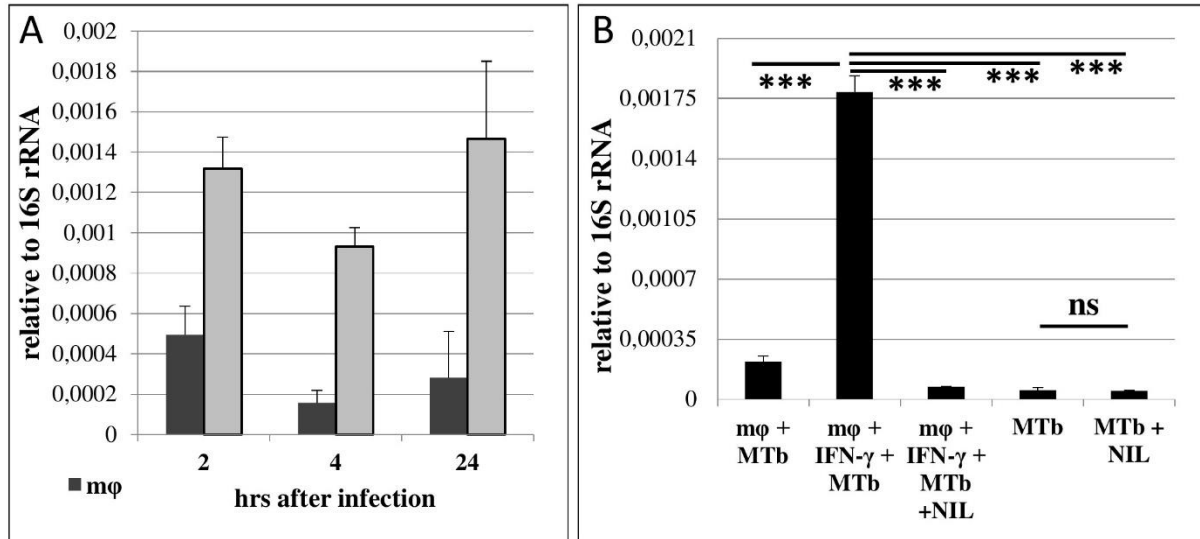
612 **Figure 1**

613

614

615

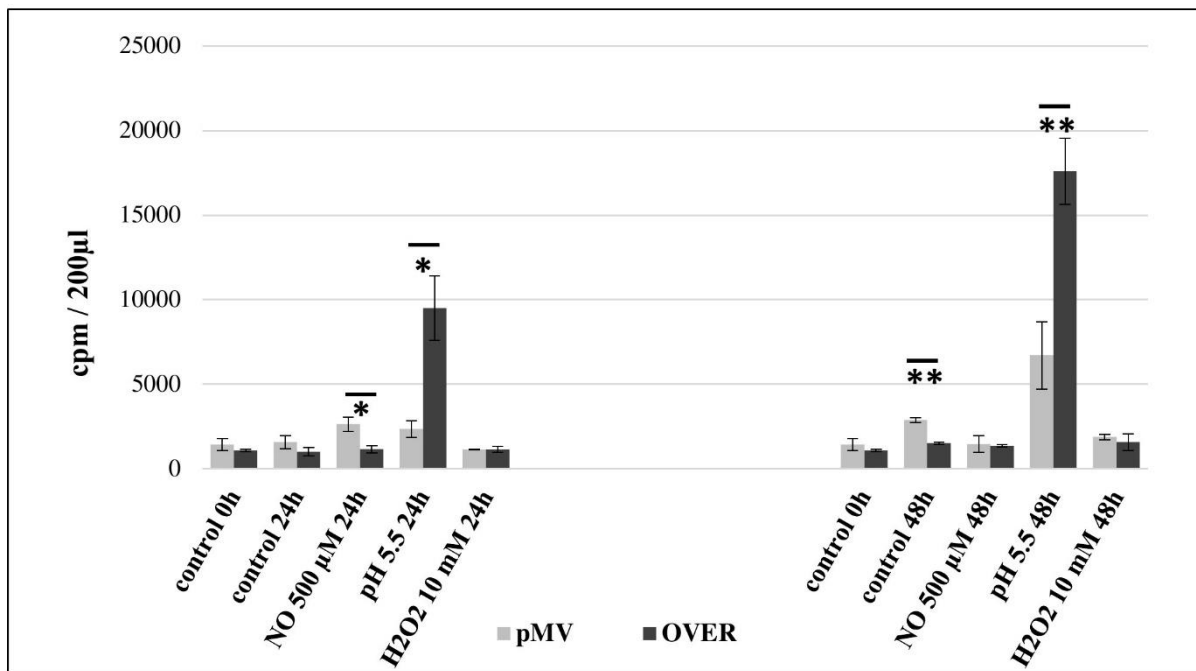
616



617

618 **Figure 2**

619



620

621 **Figure 3**

622

623